Original paper

Pertoldite, trigonal GeO$_2$, the germanium analogue of α-quartz: a new mineral from Radvanice, Czech Republic

Vladimír ŽÁČEK[1]*, Radek ŠKODA[1,2], František LAUFEK[1], Jiří SEJKORA[3], Jakub HAIFLER[1,2]

[1] *Czech Geological Survey, Klárov 3, 118 21 Praha, Czech Republic; vladimir.zacek@geology.cz*
[2] *Department of Geological Sciences, Masaryk University in Brno, Kotlářská 2, 611 37 Brno, Czech Republic*
[3] *Department of Mineralogy and Petrology, National Museum, Cirkusová 1740, 193 00 Prague 9-Horní Počernice, Czech Republic*
* *Corresponding author*

The new mineral pertoldite was found in a burning waste dump of abandoned Kateřina colliery at Radvanice near Trutnov, Hradec Králové Department, Czech Republic. The dump fire started spontaneously before 1980 and no anthropogenic material was deposited there. The determination of pertoldite as a natural analogue of synthetic trigonal α-GeO$_2$ is based on its chemical composition, X-ray powder diffraction data, and Raman spectroscopy. Pertoldite occurs as white to brownish aggregates resembling cotton tufts, up to 1 mm in size, composed of acicular crystals up to ~1 µm thick and up to 1 mm in length. Individual crystals are distorted, resembling textile fibers. Pertoldite was formed by direct crystallization from hot (400–500 °C) gasses containing Cl and F as transporting agents at a depth of 40–60 cm under the surface of a burning coal mine dump. It nucleated as a thin, delicate crust on a chip of siltstone together with multi-component aggregates of galena, stibnite, bismuthian antimony, greenockite, and bismuth. The ideal formula of pertoldite, GeO$_2$, requires 100 wt. % GeO$_2$. Germanium is partially substituted by silica (2.33–5.67 wt. % SiO$_2$), the extent of Ge$_1$Si$_{-1}$ substitution is limited to 0.03–0.09 *apfu* Si, and the empirical formula ranges between (Ge$_{0.91-0.97}$Si$_{0.03-0.09}$)$_{\Sigma 1.00}$O$_2$. Pertoldite is trigonal, *P*3$_1$21 or *P*3$_2$21, *a* = 4.980(5) Å, *c* = 5.644(4) Å, with *V* = 121.2(2) Å^3 and *Z* = 3. The strongest reflections of the powder X-ray diffraction pattern [d (Å)/I (*hkl*)] are: 4.315/44(100), 3.425/100(101,011), 2.490/31(110), 2.360/41(012,102), 1.867/31(112), 1.4179/31(023,203), 1.4124/37 (122,212). The crystal structure of pertoldite is based on corner-sharing [GeO$_4$] tetrahedra forming a three-dimensional network similar to that of α-quartz. Pertoldite is named after Zdeněk Pertold (1933–2020), professor of economic geology at the Faculty of Sciences, Charles University in Prague. The mineral and its name have been approved by the Commission on New Minerals, Nomenclature and Classification of the International Mineralogical Association (number 2021-074) and the holotype specimen is deposited in the collections in the Department of Mineralogy and Petrology, National Museum in Prague, under the catalogue number P1P 31/2021.

1. Introduction

Germanium oxide GeO$_2$ was synthetized together with other germanium compounds yet at the end of the 19th Century (Winkler 1887) and it is currently widely used in optics and electronics. Two crystalline modifications of GeO$_2$ were described. The trigonal form has an α-quartz structure (details see below), a density of 4.228 g/cm^3, a melting point of 1116 °C, and is slightly soluble in water (0.45 g/100 ml at 25 °C), soluble in HCl, HF and NaOH. The tetragonal form, described as the mineral argutite (Johan et al. 1983), has a rutile structure, density of 6.236 g/cm^3, melting point of 1086 °C, and is insoluble in water, NaOH and acids (data from Weast ed. 1979 and Lewis ed. 1993).

The first occurrence of pertoldite (as an unnamed trigonal GeO$_2$) in the burning dump of the Kateřina coal mine at Radvanice was reported by Žáček and Ondruš (1997a, b). At this time, strict rules of the IMA Commission on New Minerals and Mineral Names (Nickel

and Grice 1998) did not allow submission phases from burning dumps as valid mineral species. The recent rules – approved CNMNC-IMA proposal 16-F (Miyawaki et al. 2019) "*Crystal phases forming on the burning coaldumps with no human agency initiating the fire and no anthropogenic material deposited there should be treated as minerals*" allow to propose this phase as a new mineral. Therefore, the new mineral and the name were approved by the Commission on New Minerals, Nomenclature and Classification of the International Mineralogical Association (IMA 2021-074; Žáček et al. 2021). The holotype specimen of pertoldite is deposited in the collections in the Department of Mineralogy and Petrology, National Museum in Prague, Cirkusová 1740, 19300 Praha 9, Czech Republic, under the catalogue number P1P 31/2021. Pertoldite was named in honor of Dr. Zdeněk Pertold, CSc (1933–2020), the professor of economic geology in the Department of Geochemistry, Mineralogy and Mineral Resources of the Faculty of Sciences of the Charles University in Prague. He was an ex-

cellent teacher and expert in the field of the genesis of ore deposits, applied structural geology and ore mineralogy.

2. Occurrence

Pertoldite holotype sample was found in 1996 in "fumarole" in the central part of a burning dump of abandoned Kateřina coal mine (GPS: 50°33'39.0" N 16°03'56.2" E), situated at the eastern edge of the Radvanice village, about 12 km east of the town of Trutnov in Hradec Králové region, the Czech Republic. Radvanice is known worldwide as a unique locality with respect to the quantity and number of metal- and metalloid-bearing sublimates (Žáček and Ondruš 1997a; Žáček and Skála 2015; Sejkora et al. 2020, 2022) including radioactive galena described by Čurda et al. (2017).

From a regional geology viewpoint, the area forms a part of the Czech limb of the Intra-Sudetic Basin, which comprises continental siliciclastic sediments from early Mississippian (Namurian C) to the early Triassic age (Tásler et al. 1979). The Kateřina mine exploited six coal measures of the Stephanian B age, which were notably mineralized. The elements Pb, Zn, Cu, Cd, As, U, and the majority of sulphur were bound predominantly in minerals meanwhile, Ge, Mo, Sn, Bi, Se, Sb are postulated to be organically bound (Kudělásek 1959a, b; Čadková 1971). Increased contents of some elements in coal-bearing sediments have been studied since 1945. Besides experiments in germanium extraction, attempts to exploit uranium (mainly as uraninite and coffinite) were made in the years 1952–1957. After 1957, only coal was mined

Fig. 1 White pertoldite aggregates composed of fibers. Field of view 1 mm. Photo J. Sejkora.

again. In 1993 all mines in the Czech part of Intra-Sudetic Basin, including Radvanice, were closed, and quenching and restoration of the dump of Kateřina mine were finished in 2005. The dump fire started spontaneously in the early 1980s (Dubanský et al. 1988; 1991). Extremely high concentrations of metallic elements in coal and surrounding rocks resulted in very high contents of S, As, Se, Te, Pb, Sb, Sn, Cd, Ge, Mo and Bi in exhalations. This led to the subsequent formation of a variegated assemblage of compounds rich in these elements (Žáček and Skála 2015), which crystallized near dump surface in fissures and vents resembling volcanic fumaroles. Pertoldite was found in a "fumarole" within an area of 0.5 m^2 and about 40–60 cm under the surface of the mine dump, where the temperature reached 400–500 °C. Pertoldite is associated with multi-component aggregates containing galena, stibnite, bismuthian antimony, greenockite, and bismuth. Other germanium-bearing minerals, unnamed phases Cd_4GeS_6 and $GeAsS$, stangersite ($SnGeS_3$; Sejkora et al. 2020), and rare radvaniceite (GeS_2; Sejkora et al. 2022) crystallized above the zone with pertoldite, at slightly lower temperatures. Massive crusts reaching up to the thickness of several cm at some places, and comprising abundant salammoniac, sulphur, cryptohalite, and minor bararite, realgar, alacránite, rare bonazziite and dark orange amorphous As-rich sulphur, are developed as a lid above the horizon with germanium- and other metalloid-
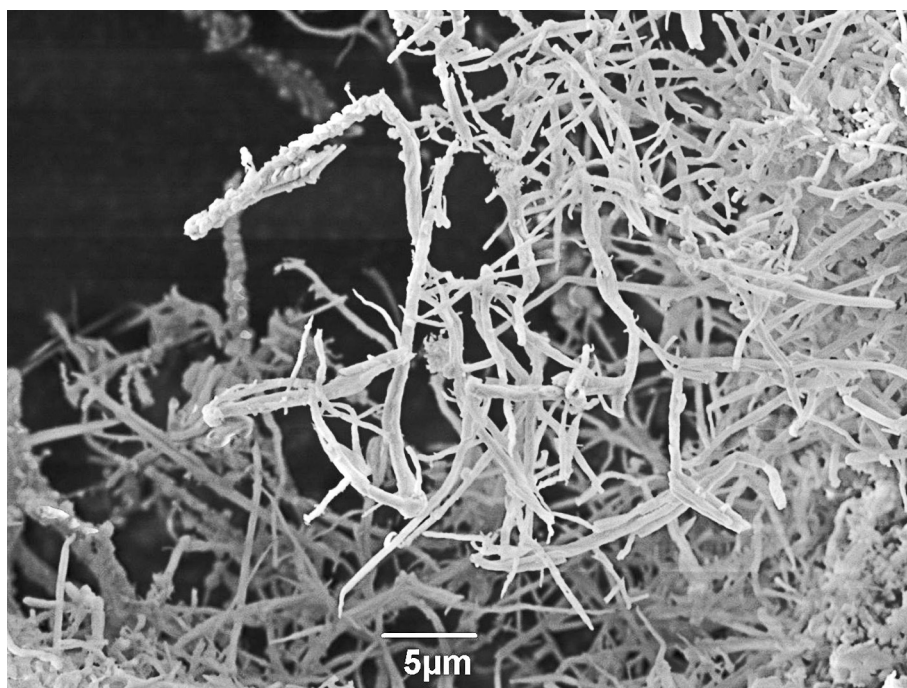

Fig. 2 The SEM photo of pertoldite aggregates. Photo R. Škoda.

bearing mineral phases (Žáček and Skála 2015). Pertoldite nucleated as a thin, delicate crust on a surface of a siltstone chip. The mineral formed by direct crystallization from hot gasses (400–500 °C; for details, see Žáček and Ondruš 1997a, or Žáček and Skála 2015), containing Cl and F as probable transporting agents.

3. Physical and optical properties

Pertoldite occurs as tiny aggregates resembling cotton tufts that are up to 1 mm in size (Fig. 1); they are composed of acicular crystals to fibers, up to ~1 μm thick and up to 1 mm in length. Individual needles are distorted and resemble textile fibers (Fig. 2). The mineral is white, with a white streak; translucent, with a silky luster. Parting and cleavage were not observed. Fluorescence was not observed at 254 and 366 nm of UV-light. The density of 4.18 g/cm³ was calculated based on the empirical formula and 4.30 g/cm³ based on the ideal formula. Hardness (Mohs and micro-indentation) could not be measured due to the cotton tuft-like feature of aggregates of fine crystals. Under the polarizing microscope, pertoldite is anisotropic and forms thin (~1 μm) distorted needles or fibers with a parallel extinction with an average refraction index $n = 1.670(5)$. Based on an empirical formula using the Gladstone-Dale constants, the mean calculated refractive index is 1.705. No pleochroism was observed. Better optical characterization was not possible due to the fine nature of the sample. The compatibility $1–(K_p/K_c)$ calculated from incomplete optical data is 0.049 (good) for the empirical formula.

4. Chemical composition

The chemical composition of pertoldite was determined from polished and carbon-coated epoxy disc, using an electron microprobe CAMECA SX100 (Masaryk University in Brno) in a wavelength-dispersive mode

and acceleration voltage of 15 kV; beam current of 5 nA, beam diameter < 1 μm. The matrix correction by X-PHI algorithm (Merlet 1994) was applied to the data. The total number of analyses is 13. The thickness of the pertoldite crystals (~1 μm) was slightly smaller than the analytical volume at 15 kV for GeO_2, which caused low analytical totals (Tab. 1); the absence of H_2O and CO_2 was confirmed by Raman spectroscopy. The concentrations of oxides normalized to 100 % vary between 94.33–97.67 wt. % GeO_2 and 2.33–5.67 wt. % SiO_2 (Tab. 1, 2). The finest analysis gave 91.20 wt. % of GeO_2 and 3.76 wt. % of SiO_2, and the total 94.96 wt. %, the empirical formula for this is $(Ge_{0.93}Si_{0.07})_{\Sigma1.00}O_2$ based on 2 oxygen atoms per formula unit. The simplified formula is $(Ge,Si)O_2$. The ideal formula is GeO_2, which requires 100 wt. % GeO_2.

Tab. 1 Chemical data of pertoldite (wt. %)

Constituent*	Range	Mean	Stand. Dev. (1σ)	Mean normalized	Range normalized
GeO₂	83.37–91.20	87.34	1.62	96.48	94.33–97.67
SiO₂	2.10–5.02	3.19	0.82	3.52	2.33–5.67
tot	88.39–94.96	90.53		100.00	100

*reference materials were metallic germanium for Ge and wollastonite for Si

Tab. 2 Representative chemical analyses of pertoldite (wt. %)

Analyzed data	1	2	3	4*	5	mean
GeO₂	88.04	90.50	90.36	91.20	89.90	87.34
SiO₂	2.10	2.31	3.67	3.76	4.42	3.19
tot	90.14	92.81	94.03	94.96	94.32	90.53
Normalized data to 100 %						
GeO₂	97.67	97.51	96.09	96.04	95.31	96.48
SiO₂	2.33	2.49	3.91	3.96	4.69	3.52
tot	100	100	100	100	100	100
Coefficients of empirical formula on the basis 2 oxygen atoms and 1 *apfu*						
Ge	0.960	0.957	0.934	0.933	0.921	0.940
Si	0.040	0.043	0.066	0.067	0.079	0.060

* – purest analysis, mean – mean was calculated from all 13 analyzes

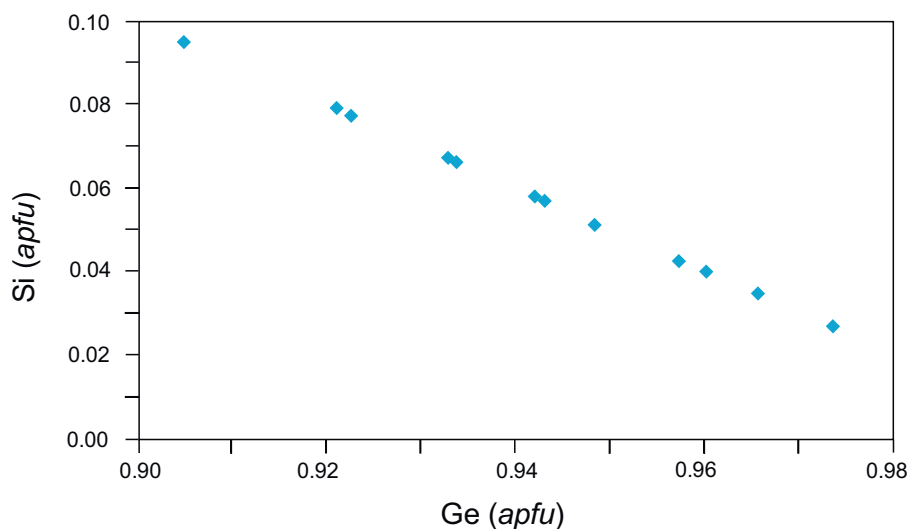**Fig. 3** The extent of Ge_1Si_{-1} substitution in pertoldite.

5. X-ray powder diffraction and crystal structure

Attempts to obtain single-crystal X-ray data were unsuccessful due to the nature of the studied material; it is formed by extremely fine fibers (Figs 1–2).

Powder X-ray diffraction (XRPD) data of pertoldite were collected in a Bragg-Brentano geometry at room temperature using a powder Bruker D8 Advance diffractometer (Czech Geological Survey). A LynxEye XE detector, Cu$K\alpha$ radiation and 10 mm automatic divergence slit were used. In order to minimize the background, the powder samples were placed on the surface of a flat silicon wafer. The powder pattern was collected in the range 5–140° 2θ, with a step of 0.015° and a counting time of 2 s per step.

The phase analysis and subsequent Rietveld analysis (Rietveld 1967, see below) revealed that the investigated sample consists of 52.6(4) wt. % of galena, 22.0(3) wt. % of greenockite, 21.0(4) wt. % of pertoldite, and 4.4(1) wt. % of antimony. Pertoldite corresponds to the trigonal GeO_2 ($P3_121$ space group, PDF-2 card no. 01-083-0543). The structure model for pertoldite was adapted for synthetic trigonal GeO_2 from Haines et al. (2002). The Rietveld refinement was performed in the Topas 5 program (Bruker AXS, 2014) using the fundamental parameter approach for the peak shape description for all phases present in the sample. Only scale factors and unit-cell parameters for all phases present in the sample were refined. CrySize L and Strain G parameters were refined for galena, whereas only refinement of CrySize L parameter was applied for greenockite and pertoldite. Because of the low antimony content, its CrySize L parameter was kept fixed during the refinement. Correction for preferred orientation (spherical harmonics function up to 6th order) of galena was applied. An attempt to refine the coordinates of pertoldite during the Rietveld refinement was made; however, the refinement did not provide reasonable values of refined coordinates of Ge and O atoms. The main reason was the relatively low pertoldite content in the sample and a partial reflection overlap with galena (e.g., 111_{galena} and $101/011_{pertoldite}$). Hence, the atomic coordinates and isotropic displacement parameters for pertoldite were taken from the trigonal GeO_2 described by Haines et al. (2002) and were fixed during the refinement. The refined unit-cell parameters are: a = 4.980(5) Å, c = 5.644(4) Å, V = 121.2(2) Å³ (Tab. 3).

The final cycles of refinement converged to residual factors R_{wp} = 0.130 and R_p = 0.104. The powder diffraction data are given in Tab. 4. It should be noted that it is impossible to distinguish between $P3_121$ (#152) and $P3_221$ (#154) space groups from powder X-ray diffraction data, thus, both space groups are possible for the pertoldite. It is also worth mentioning that the XRPD data excluded the presence of argutite, a tetragonal GeO_2, in the sample.

Tab. 4 X-ray powder diffraction data (d in Å) of pertoldite, the strongest diffractions are reported in bold

$I_{meas.}$	$d_{meas.}$	$d_{calc.}$	*$I_{calc.}$	h	k	l
44	**4.3154**	4.3128	59	1	0	0
100	**3.4251**	3.4269	100	1	0	1
		3.4269	29	0	1	1
31	**2.4896**	2.4900	6	1	1	0
41	**2.3596**	2.3615	41	0	1	2
		2.3615	5	1	0	2
29	2.2785	2.2782	43	1	1	1
23	2.1578	2.1564	39	2	0	0
31	**1.8674**	1.8672	38	1	1	2
23	1.5651	1.5661	40	1	2	1
		1.5661	2	2	1	1
31	**1.4179**	1.4177	19	0	2	3
		1.4177	12	2	0	3
37	**1.4124**	1.4115	1	1	2	2
		1.4115	38	2	1	2
21	1.2809	1.2810	1	3	0	2
		1.2810	18	0	3	2

* – intensities ($I_{calc.}$) were calculated using the software PowderCell 2.3 (Kraus and Nolze 1996) based on the crystal structure of trigonal GeO_2 (Haines et al. 2002)
** – Partial overlap with 100 galena reflection

Pertoldite adopts the crystal structure of the trigonal synthetic GeO_2 structure. This structure was first solved by Smith and Isaacs (1964). Subsequently, the structure has been refined several times by, e.g., Yamanaka and Ogata (1991), Glinnemann et al. (1992) and more recently using neutron diffraction data of Haines et al. (2002). The crystal structure of pertoldite is based on corner-sharing $[GeO_4]$ tetrahedra forming a three-dimensional network (Fig. 4). Its crystal structure is very similar to that of α-quartz, although there are some structural differences. The GeO_4 tetrahedra in pertoldite are more distorted than the corresponding SiO_4 tetrahedra in α-quartz. The O–Ge–O angles in GeO_4 tetrahedra in pertoldite show range from 106.3° to 113.1°. In the α-quartz structure, the corresponding SiO_4 tetrahedra are more uniform, with the O–Si–O angles ranging from 108.3° to 110.7°. The corresponding Si–O–Si and Ge–O–Ge angles also differ in both structures; they are 130.1° and 144.0° for α-quartz and pertoldite, respectively (Jorensen 1978; Micoulaut et al. 2006).
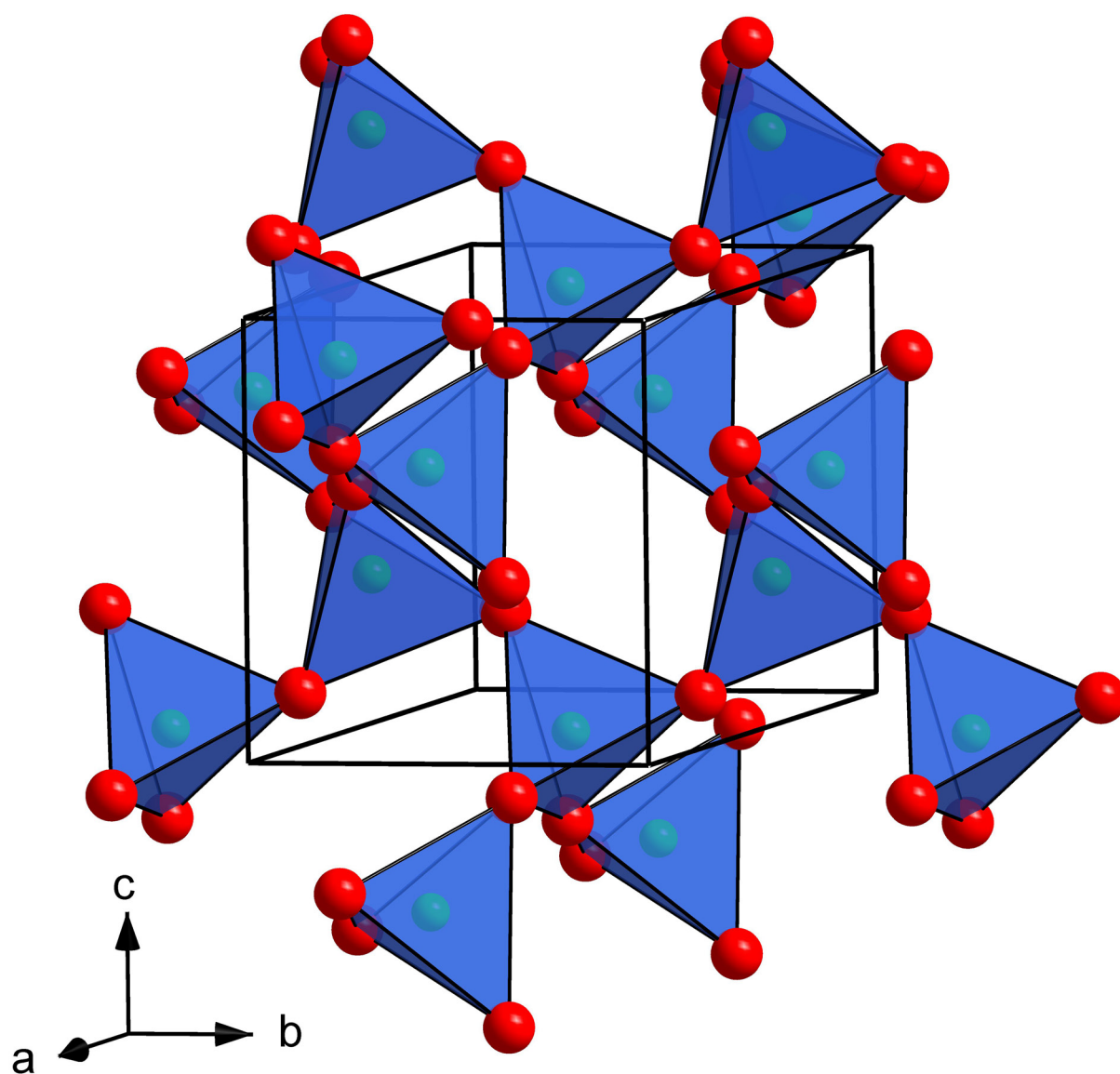
Tab. 3 Unit-cell parameters of pertoldite and synthetic GeO_2, trigonal $P3_121$, Z = 3

	reference	a [Å]	c [Å]	V [Å³]
pertoldite[1]	this paper	4.980(5)	5.644(4)	121.2(2)
pertoldite[2]	Žáček and Ondruš (1997b)	4.982(6)	5.65(1)	121.4(4)
synthetic GeO_2	Haines et al. (2002)	4.98503(3)	5.64711(4)	121.532(1)

[1] – holotype specimen Ra101; [2] – described as unnamed GeO_2

Fig. 4 The crystal structure of trigonal GeO$_2$ showing corner-sharing [GeO$_4$] tetrahedra, based on the data of Haines et al. (2002). Red and green spheres are oxygen and germanium atoms, respectively.

6. Raman spectroscopy

The Raman spectra of pertoldite were collected in the range 30–3600 cm^{-1} using a DXR dispersive Raman Spectrometer (Thermo Scientific) mounted on a confocal Olympus microscope (Department of Mineralogy and Petrology, National Museum, Prague). The Raman signal was excited by an unpolarised green 532 nm solid state, diode-pumped laser, and detected by a CCD detector. The experimental parameters were: 100× objective, 10 s exposure time, 100 exposures, 50 μm pinhole spectrograph aperture, and 10 mW laser power level. Any possible eventual thermal damage of the measured areas was excluded by visual inspection of the excited surface after measurement, by observation of possible decay of spectral features at the start of excitation, and by checking the thermal downshift of the Raman bands. The instrument was set up by a software-controlled calibration procedure using multiple neon emission lines (wavelength calibration), multiple polystyrene Raman bands (laser frequency calibration), and standardized white-light sources (intensity calibration). Spectral manipulations were performed using the Omnic 9 software (Thermo Scientific). The Raman spectrum of pertoldite is given in Fig. 5. The main
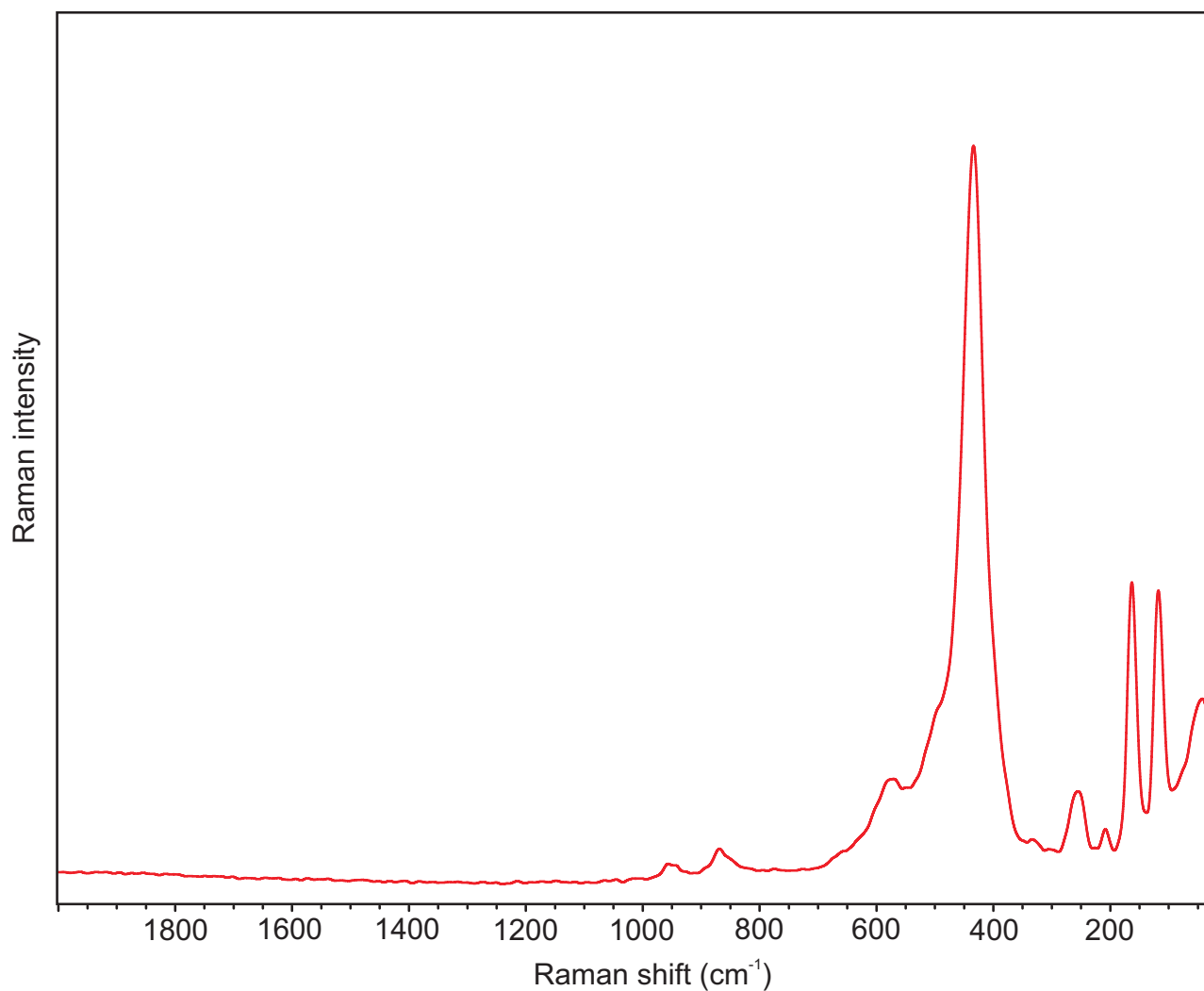
Fig. 5 Raman spectrum of pertoldite in the range 2000–30 cm^{-1}.

Tab. 5 Comparison of Raman wavenumbers of pertoldite and synthetic trigonal GeO$_2$

this paper	Scott (1970)	Gillet et al. (1990)	Micoulaut et al. (2006)	assignment
	972	970	973	*E* mode (*LO*)
956	961	961	960	*E* mode (*TO*)
943	949	949		*E* mode (*LO*)
869	880	880	881	*A*$_1$ mode
853	857	857	860	*E* mode (*TO*)
582	595	595	593	*E* mode (*LO*)
574	583	583	583	*E* mode (*TO*)
	512	514	516	*E* mode (*LO*)
497	492	492		*E* mode (*TO*)
	456	456		*E* mode (*LO*)
433	440	442	444	*A*$_1$ mode
	385	385		*E* mode (*TO*)
	372	372		*E* mode (*LO*)
333	326	327	330	*E* mode (*TO*)
255	261	261	263	*A*$_1$ mode
209	212	212	213	*A*$_1$ mode
164	166	164	166	*E* modes (*TO+LO*)
118	121	122	123	*E* modes (*TO+LO*)
41				lattice vibration

bands observed are (in wavenumbers): 956, 943, 869, 853, 582, 574, 497, 433, 333, 255, 209, 164, 118, and 41 cm^{-1}. The experimental spectrum agrees very well with published Raman spectra of synthetic α-quartz modification of GeO_2 (Tab. 5) and distinctly differs from data of tetragonal rutile-like GeO_2 (e.g., Scott 1970; Gillet et al. 1990; Micoulaut et al. 2006). The Raman spectrum of pertoldite exhibits four symmetric modes of A_1 symmetry and eight doubly degenerate modes of E symmetry, all split into transverse optic (*TO*) and longitudinal optic modes (*LO*) (Scott 1970; Gillet et al. 1990; Micoulaut et al. 2006). The bands at 209, 255, 433, and 869 cm^{-1} are attributed to the A_1 modes. The E modes are represented by the following bands at 118 (*TO+LO*), 164 (*TO+LO*), 333 (*TO*), 497 (*TO*), 574 (*TO*), 582 (*LO*), 853 (*TO*), 943 (*LO*), and 956 (*TO*) (Scott 1970; Dultz et al. 1975; Gillet et al. 1990; Micoulaut et al. 2006).

7. Origin and relation to other species

Crystalline GeO_2 occurs at ambient temperature and pressure as two polymorphs: as α-quartz-like trigonal structure (space group $P3_221$) and as rutile-like tetragonal structure (space group $P4_2/mnm$); Micoulaut et al. 2006). The tetragonal GeO_2 is known as the mineral argutite, which forms microscopic inclusions in sphalerite in a zinc deposit in metamorphosed Lower Paleozoic sediments from the Argut, central Pyrenees, Haute-Garonne, France (Johan et al. 1983).

The modification of GeO_2, stable at room temperature, is the tetragonal polymorph with rutile-like structure, which transforms into the α-quartz-like structure at 1008 °C (Yamanaka and Ogata 1991). The rutile-based structure is also stabilized under high-pressure (Yamanaka and Ogata 1991). According to Haines et al. (2002), the trigonal polymorph is metastable under ambient conditions and can be obtained by cooling from above 1036 °C and from direct synthesis from various precursors, such as hydrolysis of $GeCl_4$. Data on the occurrence of $GeCl_4$ within the coal-fire vapors is given by Kruszewski et al. (2018b). Balitsky et al. (2001) reviewed low-temperature methods used for the preparation of synthetic α-quartz GeO_2 and designed a new refluxed method for growing its single crystals.

Pertoldite chemical analysis shows elevated content of SiO_2 (~3.4 wt. % SiO_2). The presence of cryptohalite and bararite [both $(NH_4)_2SiF_6$)] crusts at the colder places of the "fumarole vent" above the pertoldite, give evidence for the presence of Si complexes in the hot gasses from which pertoldite crystallized (cf. Laufek et al. 2017; Kruszewski et al. 2018b, 2020). Silicon probably enters the pertoldite structure via homovalent substitution $Si^{4+}_1Ge^{4+}_{-1}$. An extensive solid solution of α-GeO_2 and

α-SiO_2 has been studied on synthetic samples by Balitsky et al. (2001, 2005).

Germanium is compatible with rock-forming minerals and substitutes for Si due to its similar ionic radius and the same charge. Although the bulk content of Ge in common rocks varies from ~0.1 to ~2.5 ppm (Bernstein 1985; Höll et al. 2007), the slightly elevated content was determined in fractionated granitic rocks (≤ 8.8 ppm; Breiter et al. 2013). Germanium can be substantially accumulated in some sulphidic deposits (e.g., Tsumeb, Namibia), coal, organic matter, and petrified wood (Bernstein 1985; Höll et al. 2007, see also Seredin and Finkelman 2008). The extreme concentrations of Ge (up to 11 000 ppm) recorded in fly ashes originated from the Ge-enriched coal (Höll et al. 2007, cf. Bouška 1981). The coal from the Radvanice is also substantially enriched in Ge (average 192 ppm, maximum 940 ppm in ash; Pešek et al. 2010). Hence, the spontaneous combustion of Ge-enriched coal in Radvanice coal dump established conditions, such as high Ge content, high temperature, suitable Cl and F transporting agents, possibly $GeCl_4$, mentioned by Kruszewski et al. (2018b), or NH_4Cl, determined experimentally by Laufek et al. (2017), with omnipresent sulphur and NH_3, eligible for pertoldite formation. Finally, it should be mentioned that germanium is rarely found deposited within the minerals of the burning coal-mine heaps. Only Kruszewski (2018a) reported germaniferous cuspidine (895 ppm Ge) among neo-formed minerals of the Lower Silesian Basin in Poland. Pertoldite, and other germanium-containing species from Radvanice, are thus an important exception.

References

Balitsky DV, Balitsky VS, Pisarevsky YV, Philippot E, Silvestrova OY and Pushcharovsky DY (2001) Growth of germanium dioxide single crystals with α-quartz structure and investigation of their crystal structure, optical, elastic, piezoelectric, dielectric and mechanical properties. Ann Chim-Sci Mat 26(1): 183–192

Balitsky VS, Balitsky DV, Nekrasov AN, Balitskaya LV (2005) Growth and characterization of Si$_x$Ge$_{1-x}$O solid solution single crystals with quartz structure. J Cryst Growth 275(1–2): e807–e811

Bernstein L R (1985) Germanium geochemistry and mineralogy. Geochim Cosmochim Acta 49(11): 2409–2422

Bouška V (1981) Coal Science and Technology 1, Geochemistry of Coal. Elsevier, Amsterdam, pp 1–284

Breiter K, Gardenová N, Kanický V, Vaculovič T (2013) Gallium and germanium geochemistry during magmatic fractionation and post-magmatic alteration in different types of granitoids: A case study from the Bohemian Massif (Czech Republic). Geol Carpath 64(3), 171

Bruker AXS (2014) Topas 5, computing program, Bruker AXS GmbH, Karlsruhe, Germany

Čadková Z (1971) The metal distribution in sediments of the Radvanice measures. Čas Mineral Geol 16(2): 147–157 (in Czech)

Čurda M, Goliáš V, Klementová M, Strnad L, Matěj Z, Škoda R (2017) Radiation damage in sulfides: Radioactive galena from burning heaps, after coal mining in the Lower Silesian basin (Czech Republic). Amer Miner 102(9): 1788–1795

Dubanský A, Absolon K, Dvořáček (1988) Selenium from burning dumps of the Stachanov mine. Geol Průzk 3: 308–309 (in Czech)

Dubanský A, Langrová A, Dvořáček P, Čejka J, Kouřimský J (1991) Pyrometamorphic minerals from the Kateřina mine. Geol Průzk 6: 172–173 (in Czech)

Dultz W, Quilichini M, Scott JF, Lehmann G (1975) Phonon spectra of quartz isomorphs. Phys Rev B 11(4): 1648

Gillet P, Le Cléac'h A, Madon M (1990) High-Temperature Raman spectroscopy of SiO_2 and GeO_2 Polymorphs: Anharmonicity and thermodynamic properties at high-temperatures. J Geophys Res B: Solid Earth 95(B13), 21635–21655

Glinnemann J, King HE, Schulz H, Hahn T, la Placa SJ, Dacol F (1992) Crystal structures of the low-temperature quartz-type phases of SiO_2 and GeO_2 at elevated pressure. Z Kristallogr 198: 177–212

Haines J, Cambon O, Philippot E, Chapon L, Hull S (2002) A Neutron Diffraction Study of the Thermal Stability of the α-Quartz-Type Structure in Germanium Dioxide. J Solid State Chem 166: 434–441

Höll R, Kling M, Schroll E (2007) Metallogenesis of germanium – A review. Ore Geol Rev 30 (3–4): 145–180

Johan Z, Oudin E, Picot P (1983) Analogues germaniféres et galliféresdes silicates et oxydes dans les gisements de zinc des Pyrénées centrales, France; argutite et carboirite, deux nouvelles espéces minérales. Tschermaks mineral petrogr Mitt 31: 97–119

Jorensen JD (1978) Compression mechanisms in α-quartz structures – SiO_2 and GeO_2. J Appl Phys 49: 5473–8

Kraus W, Nolze G (1996) POWDER CELL – a program for the representation and manipulation of crystal structures and calculation of the resulting X-ray powder patterns. J Appl Crystallogr 29: 301–303

Kruszewski Ł (2018a) Geochemical Behavior of Trace Elements in the Upper and Lower Silesian Basin Coal-Fire Gob Piles of Poland. Chapter 19. In: Stracher GB, Prakash A, Sokol EV (Eds) Coal and Peat Fires: A Global Perspective, Volume 5 Case Studies-Advances in Field and Laboratory Research. Elsevier, Amsterdam, pp 107–449

Kruszewski Ł, Fabiańska MJ, Ciesielczuk J, Segit T, Orłowski R, Motyliński R, Kusy D, Moszumańska I (2018b) First multi-tool exploration of a gas-condensate-pyrolysate system from the environment of burning coal mine heaps: An in situ FTIR and laboratory GC and PXRD study based on Upper Silesian materials. Sci Total Environ 640–641: 1044–1071

Kruszewski Ł, Fabiańska MJ, Segit T, Kusy D, Motyliński R, Ciesielczuk J, Deput E (2020) First multi-tool exploration of a gas-condensate-pyrolysate system from the environment of burning coal mine heaps: An in situ FTIR and laboratory GC and PXRD study based on Upper Silesian materials. Sci Total Environ 698: 134274

Kudělásek V (1959a) Trace elements of coal of the Intra-Sudetic Basin. Part I. Sbor věd Prací Vys Šk báň (Ostrava), Ř horn-geol 5(3): 319–347 (in Czech)

Kudělásek V (1959b) Trace elements of coal of the Intra-Sudetic Basin. Part II. Sbor věd Prací Vys Šk báň (Ostrava), Ř horn-geol 5(4): 457–479 (in Czech)

Laufek F, Veselovský F, Drábek M, Kříbek B, Klementová M (2017) Experimental formation of Pb, Sn, Ge and Sb sulfides, selenides and chlorides in the presence of sal ammoniac: A contribution to the understanding of the mineral formation processes in coal wastes self-ignition. Int J Coal Geol 176–177: 1–7

Lewis RJ Sr., ed (1993) Hawley's Condensed Chemical Dictionary. 12th ed. New York, NY: Van Nostrand Rheinhold Co

Merlet C (1994) An Accurate Computer Correction Program for Quantitative Electron Probe Microanalysis. Microchim Acta 114/115: 363–376

Micoulaut M, Cormier L, Henderson GS (2006) The structure of amorphous, crystalline and liquid GeO_2. J Phys: Condens Matter 18 (45): R753–R784

Miyawaki R, Hatert F, Pasero M, Mills SJ (2019) IMA Commission on New Minerals, Nomenclature and Classification (CNMNC), NEWSLETTER 50 New minerals and nomenclature modifications approved in 2019. Mineral Mag 83: 615–620

Nickel EH, Grice JD (1998) The IMA Commission on New Minerals and Mineral Names: procedures and guidelines on mineral nomenclature. Mineral Petrol 64(1–4): 237–263

Pešek J, Sýkorová I, Jelínek E, Michna O, Forstová J, Martínek K, Vašíček M, Havelcová M (2010): Major and minor elements in the hard coal from the Czech Upper Paleozoic basins. Czech Geol Surv Spec Pap 10: 1–48

Rietveld HM (1967) Line profiles of neutron powder-diffraction peaks for structure refinement. Acta Crystallogr 22: 151–152

Scott JF (1970) Raman Spectra of GeO₂. Phys Rev B 1(8): 3488–3493

Sejkora J, Makovicky E, Balić-Zunić T, Berlepsch P (2020) Stangersite, a new tin germanium sulfide, from the Kateřina mine, Radvanice near Trutnov, Czech Republic. J Geosci 65(3): 141–152

Sejkora J, Žáček V, Škoda R, Laufek F, Dolníček Z (2022): Radvaniceite, GeS₂, a New Germanium Sulphide, from the Kateřina Mine, Radvanice near Trutnov, Czech Republic. Minerals 12: 222

Seredin VV, Finkelman RB (2008): Metaliferous coals: A review of the main genetic and geochemical types. Int J Coal Geol 76,4: 253–289

Smith GS, Isaacs PB (1964) The crystal structure of quartz-like GeO₂. Acta Crystallogr 17: 842–846

Tásler R, Čadková Z, Dvořák J, Fediuk F, Chaloupský J, Jetel J, Kaiserová-Kalibová M, Prouza V, Schovánková-Hrdličková D, Středa J, Střída M, Šetlík J (1979) Geology of Czech part of the Intrasudetic Basin. Academia, Praha, pp 1–292 (in Czech)

Weast RC, ed (1979) Handbook of Chemistry and Physics. 60th ed. Boca Raton, Florida: CRC Press Inc

Winkler C (1887) Mittheilungen über des Germanium. Zweite Abhandlung. J Prakt Chem 36(1): 177–209

Yamanaka Y, Ogata K (1991) Structure Refinement of GeO₂ Polymorphs at High Pressures and Temperatures by Energy-Dispersive Spectra of Powder Diffraction. J Appl Crystallogr 24: 111–118

Žáček V, Ondruš P (1997a) Mineralogy of recently formed sublimates from Kateřina colliery in Radvanice, Eastern Bohemia, Czech Republic. Bull Czech Geol Surv 72(3): 289–302

Žáček V, Ondruš P (1997b) Naturally occurring germanium compounds, GeSnS₃ and GeO₂ from Radvanice, Eastern Bohemia. Bull Czech Geol Surv 72(2): 189–191

Žáček V, Skála R (2015) Mineralogy of Burning-Coal Waste Piles in Collieries of the Czech Republic. In: Stracher GB, Prakash A, Sokol EV Coal and Peat Fires: A Global Perspective, Volume 3 Case Studies-Coal Fires. Elsevier, Amsterdam, pp 109–159

Žáček V, Škoda R, Laufek F, Sejkora J, Haifler J (2021) Pertoldite, IMA 2021-074. CNMNC Newsletter 64. Eur J Mineral 33, 139–143